Imaging probes and modalities for the study of Solute Carrier O (SLCO)-transport function in vivo

Solène Marie, Salvatore Cisternino, Irene Buvat, Xavier Declèves, Nicolas Tournier

Imaging probes and modalities for the study of Solute Carrier O (SLCO)-transport function *in vivo*

Solène Marie[1,2,3], Salvatore Cisternino[4,5], Irène Buvat[1], Xavier Declèves[4,5], Nicolas Tournier[1,*]

1. Imagerie Moléculaire In Vivo, IMIV, CEA, Inserm, CNRS, Univ. Paris-Sud, Université Paris Saclay, CEA-SHFJ, Orsay F-91401, France
2. AP-HP, Hôpital Bicêtre, Pharmacie Clinique, Le Kremlin Bicêtre, France
3. Univ Paris-Sud, Faculté de Pharmacie, Châtenay-Malabry, F-92296, France
4. Variabilité de réponse aux psychotropes, INSERM, U1144, Paris, France
5. Université Paris Descartes, Faculté de pharmacie, UMR-S 1144, Paris, F-75006, France.

* **Corresponding author:** Dr Nicolas Tournier (PhD, PharmD)

nicolas.tournier@cea.fr

CEA, DRF, ISVFJ, IMIV, Service Hospitalier Frédéric Joliot, Orsay, F-91401, France

Phone number: +33 1 69 86 77 12 Fax number: +33 1 69 86 77 68

Number of words

- Whole manuscript: 7,287
- Abstract: 150
- 27 pages, 5 figures, 2 tables

Running Title: Imaging SLCO-transport function *in vivo*

Abstract

Transporters of the Solute Carrier O (SLCO) family, former organic anion-transporting polypeptides (OATP), are now recognized as key players in pharmacokinetics. Imaging is increasingly regarded as a relevant method to elucidate and decipher the intrinsic role of SLCO in controlling drug disposition in plasma and tissues. Current research in this representative field of translational research is based on different imaging modalities including nuclear imaging, such as Single Photon Emission Computed Tomography (SPECT) or Positron Emission Tomography (PET), as well as Magnetic Resonance Imaging (MRI). Imaging modalities can be compared in terms of sensitivity, quantitative properties, spatial resolution, variety of ligands and radiation exposure. All of these approaches rely on the use of SLCO-substrates that are detected using corresponding modalities. The present review aims at reporting and comparing the imaging probes that have been proposed to study SLCO-transport function, in terms of *in vitro* specificity, *in vivo* behavior and clinical validation.

Keywords: Solute transporters, Organic anion-transporting polypeptide transporters, Imaging methods, Hepatic transport

Introduction

Membrane transporters are now recognized as key players in pharmacokinetics (PK). Each transporter has a specific pattern of substrates and tissue expression. Transporters of the ATP-binding cassette (ABC) and solute carrier (SLC) superfamilies expressed in the intestine, liver, and kidneys have been shown to control the absorption, distribution and/or elimination of many drugs and measurably impact PK. Transporter function is also assumed to account for intra- and inter-individual variability in drug PK[1]. Many clinically relevant drug-drug interactions (DDI) involving transporter inhibitors, inducers and substrates have been described[2]. In 2007, the International Transporter Consortium (ITC), which includes members from academia, industry, and the US Food and Drug Administration (FDA), was formed with the goal of determining transporters that are of emerging importance, establishing recommendations, regulatory draft guidance documents on transporter–drug interactions, and highlighting transporter-related challenges in drug development[1,3]. In this framework, imaging is increasingly regarded as a safe and relevant method to elucidate and decipher the intrinsic role of membrane transporters in controlling drug disposition[4].

Transporters expressed in blood-tissue barriers have been shown to control the tissue exposure to many compounds[2]. These transporters may control the drug tissue distribution with limited impact on the plasma PK. In this framework, several imaging methods have been proposed to non-invasively unveil and quantify the impact of transporter function on drug exposure to non-clearance organs such as the blood-brain barrier[5–7], the blood-retina barriers[8] or the blood-tumor barrier[9] in animals and/or humans.

The solute carrier O (SLCO) transporter family

Among SLC transporters, the Solute Carrier O (SLCO) transporter family has been detected at many blood-tissue interfaces[10]. SLCO were initially identified at the basolateral membrane of hepatocytes where they mediate the transport of bile salt and cholephilic anionic compounds[10] (Figure 1).

Today, 11 members of the SLCO family have been identified in Human[11]. This superfamily was originally named Organic Anion-Transporting Polypeptides (OATP) or SLC21A. The nomenclature of its members was then updated and standardized and the superfamily was renamed to SLCO, the solute carrier family of the OATP. Based on their amino acid sequence identities, the different SLCOs cluster into families, in general with more than 40% amino acid sequence identity[10] (Table 1). The different proteins are named SLCO (Slco for the rodent proteins) followed by the family number (SLCO1, SLCO2, SLCO3, SLCO4, SLCO5, and SLCO6), the subfamily letter (e.g. SLCO1A, SLCO1B) and then a consecutive number to identify the individual members within the family (e.g. Slco1a1, SLCO1A2 and Slco1a3). The corresponding gene symbols are SLCO followed by the same number–letter–number combination in italic type (e.g. *Slco1a1*, *SLCO1A2* and *Slco1a3*)[12].

Direct comparisons between human (SLCO) and rodent (Slco) studies is difficult, due to numerous gene duplication and divergence that occurred in this family, especially in rodents. Moreover, several aliases and former names of the different SLCO members co-exist in the literature (e.g. OATP-B, OATP8), which complicates the understanding and comparison of previously reported data (Table 1).

SLCO1B1 and SLCO1B3 have a single rodent orthologue, Slco1b2. Human SLCO1A2 has five rodent orthologues: Slco1a1, Slco1a3 (in rats only), Slco1a4, Slco1a5 and

Slco1a6. The other human SLCOs and their respective rodent orthologues are SLCO1C1 (Slco1c1), SLCO2A1 (Slco2a1), SLCO2B1 (Slco2b1), SLCO3A1 (Slco3a1), SLCO4A1 (Slco4a1), SLCO4C1 (Slco4c1), SLCO5A1 and SLCO6A1 (Slco6b1, Slco6c1 and Slco6d1)[12] (Table 1).

The expression of SLCO transporters has been mainly detected in epithelial and endothelial cell membranes of many organs[11,13]: some SLCO isoforms have a restricted expression and are considered as organ-specific, like SLCO1B1 and SLCO1B3 that are assumed to be liver-specific[12,13] (Figure 1). Due to their broad specificity and the number of known DDIs, liver uptake transporters SLCO1B1 and SLCO1B3 have been deemed clinically relevant by most regulatory agencies[1]. It is now mandatory to investigate SLCO1B1 and SLCO1B3 substrate or inhibitor potential of any new chemical entity during the drug development. This systematic screening, in addition to academic research, highlighted the high prevalence of SLCO1B1/1B3-substrates from various chemical and pharmacological families[12,14]. This suggests that the relative importance of carrier-mediated uptake by the liver, as a prerequisite for the hepatic clearance of many drugs, may have been underestimated[11].

SLCO2B1 is localized at both the sinusoidal membrane of hepatocytes (Figure 1) and apical membrane of enterocytes and mediates the absorption and the liver uptake of its substrates[15,16]. In addition to the intestine and liver, SLCO2B1 expression was also detected in human small arteries and vein of the heart, blood-brain barrier, epithelial lung cells, ovary, myoepithelium of mammary duct, prostate, kidney, platelets, skeletal muscle and placenta[10]. Other SLCO transporters are largely expressed such as SLCO1A2, SLCO2A1, SLCO3A1 and SLCO4A1 that have been detected in a broad number of tissues[12,13]. SLCO1A2 might play a role in intestinal absorption. SLCO1A2

expression was also detected at the blood-brain barrier, kidney, intestine, cholangiocytes and eye ciliary body[10].

This ubiquitous distribution at many blood-tissue interfaces, not only of absorption or clearance organs, suggests a functional role for these extrahepatic SLCO transporters in controlling the access of drugs to target and/or vulnerable tissues, with consequences on drug efficacy or safety[2]. SLCO function may thus be hypothesized to account for pharmacodynamics by influencing cellular drug accumulation in relevant target tissues.

Imaging SLCO transporter function

Non-invasive approaches are therefore required to elucidate or predict the impact of SLCO-mediated transport in clearance organs on drug disposition in plasma. Moreover, imaging methods would be useful to unveil and quantify the role of non-hepatic SLCO transporter function on drug distribution in organs, as a prerequisite to the local pharmacological/toxicological effect. In the absence of measurable concentration in tissues, conventional PK approaches do not allow for investigating the role of SLCO transporters at the blood-tissue interface. Data are limited to those obtained in invasive and terminal studies in animals or cellular models. However, extrapolation of results obtained from rodents to humans is difficult due to the lack of direct orthology between rodent and human SLCO isoforms [12,17] (Table 1), together with species differences regarding substrate specificity and tissue expression[18].

The development of imaging probes and methodologies dedicated to the study of SLCO-transport function *in vivo* represents a major challenge to decipher the role of this specific transporter family and address its impact for pharmacotherapy. Current research in this representative field of translational research is based on different

imaging modalities (Figure 2). This includes nuclear imaging such as Single Photon Emission Computed Tomography (SPECT) or Positron Emission Tomography (PET)[19], as well as Magnetic Resonance Imaging (MRI). All of these approaches rely on the use of SLCO-substrates that are detected using corresponding modalities. Imaging modalities can be compared in terms of sensitivity, quantitative properties, spatial resolution, variety of ligands and radiation exposure (Figure 2).

Pr. Yiuchi Sugiyama and coworkers have performed pioneer work on the use of PET imaging for the study of SLCO transport function *in vivo*. They have paved the way for an extensive and inspiring translational research which contributed to highlight the importance of SLCO function for modern PK[20,21]. The present review aims at reporting the current knowledge regarding imaging probes and modalities that have been proposed to study SLCO-transport function *in vivo*. The approaches are compared in terms of *in vitro* specificity, *in vivo* behavior and clinical validation.

Imaging probes for SPECT

SPECT uses gamma rays detected by gamma cameras that have been readily available in most nuclear medicine departments for decades. The radionuclide gamma emitter most frequently used is metastable technetium-99 (^{99m}Tc) because of its medium energy (140 keV), relatively short half-life ($T_{1/2}$ = 6.0 hours) and availability through the molybdene-technetium generator. ^{99m}Tc is a radionuclide that requires forming an organic coordination complex, limiting the possibility to radiolabel substrates without dramatic changes in their chemical and physico-chemical properties[22]. However, ^{99m}Tc allows for easy and kit-based preparation of radiopharmaceutical agents for human use and often provides suitable metabolic

stability *in vivo*. Several other radionuclides are eligible to SPECT, including iodine-123 or indium-111.

SPECT has traditionally been deemed a non-quantitative imaging method. However, recent advances in medical physics have now made SPECT a quantitative method thanks to coupling with a CT scan (Computed Tomography) in hybrid SPECT/CT scanners, advances in algorithms for image reconstruction and sophisticated compensation techniques to correct for photon attenuation and scattering[23]. Quantification with SPECT however remains of slightly lower performance than with PET, especially in small volume regions, due to marginally poorer image spatial resolution (typically ~7-10 mm for SPECT against ~5-8 mm for PET, depending on the image reconstruction parameters)[23]. SPECT benefits from a good sensitivity, allowing for the use of tracer dose compounds, with a limited risk of toxicity (Figure 2).

^{99m}Tc-mebrofenin

SLCO-function has been studied in SPECT imaging using ^{99m}Tc-mebrofenin, an imino diacetic acid (HIDA) derivative (Figure 3) commonly used in nuclear medicine for hepatobiliary scintigraphy. *In vitro* studies with *xenopus laevis* oocytes[24,25] and chinese hamster ovary cells[25,26] have shown that ^{99m}Tc-mebrofenin is transported by human SLCO1B1 and SLCO1B3 but not SLCO2B1[25]. ^{99m}Tc-mebrofenin is not either a substrate of the Na^+-taurocholate co-transporing polypeptide (NTCP, SLC10A1) expressed at the hepatocyte level[25] (Figure 1). The critical role played by these transporters in the liver kinetics of ^{99m}Tc-mebrofenin has been highlighted *in vivo* using Slco1a/1b (*Slco1a*$^{-/-}$*/1b*$^{-/-}$) mice or using rifampicin, a potent SLCO inhibitor[26]. Regarding efflux transporters of the ABC superfamily, ^{99m}Tc-mebrofenin is transported by ABCC2 (multidrug resistance protein 2, MRP2)[24,27,28] and ABCC3 (MRP3)[24].

Studies in Abcc2-deficient mice have unveiled the contribution of Abcc2 to the biliary secretion of ^{99m}Tc-mebrofenin[26]. In mice, rifampicin was shown to impact both the Slco-mediated liver uptake and the Abcc2–mediated biliary efflux of ^{99m}Tc-mebrofenin[26] (Figure 1, Table 2).

A PK study was conducted in healthy volunteers, consisting in a model developed on blood, urine and bile concentration-time profiles[24]. It unveiled the predominant biliary route of excretion, compared to the urinary route[24] which represents 1% of total clearance under normal conditions. ^{99m}Tc-mebrofenin has been used for decades as an approved radiopharmaceutical agent to assess altered hepatobiliary function in patients[24]. However, to the best of our knowledge, the respective impact of the different SLCO isoforms on ^{99m}Tc-mebrofenin liver kinetics in humans has not been reported.

^{99m}Tc-N-pyridoxyl-5-methyltryptophan

^{99m}Tc-N-pyridoxyl-5-methyltryptophan (^{99m}Tc-PMT) is a radiotracer among the ^{99m}Tc-pyridoxylaminate family (Figure 3). ^{99m}Tc-PMT has been approved in Japan to perform hepatobiliary scintigraphy to diagnose diseases of the hepatobiliary function and system[29–31]. A recent *in vitro* study aimed at elucidating the transport mechanisms involved in the hepatic uptake of ^{99m}Tc-PMT. The authors showed that ^{99m}Tc-PMT is transported by SLCO1B1 and SLCO1B3 *in vitro*[32]. There was no difference in the uptake of ^{99m}Tc-PMT in SLCO2B1, SLC22A1 (Organic cation transporter 1, OCT1) and SLC22A7 (Organic anion transporter 2, OAT2)-expressing cells compared with control cells[32]. The *in vivo* importance and specificity of the SLCO transport of ^{99m}Tc-PMT have not been explored yet. ^{99m}Tc-PMT may nonetheless represent an alternative to ^{99m}Tc-mebrofenin.

.[111]In-EOB-DTPA

[111]In-EOB-DTPA is an experimental SPECT tracer derived from the MRI contrast agent Gd-EOB-DTPA (gadolinium-ethoxybenzyl-diethylenetriamine-pentaacetic acid; Figure 3). [111]In-EOB-DTPA has been used in mice to validate an original gene reporter system based on the expression of Slco1a1 by a transfected xenograft[33]. A signal enhancement was observed using both [111]In-EOB-DTPA and Gd-EOB-DTPA (MRI probe, see below) in Slco1a1-expressing xenograft compared to control xenograft, that did not express this transporter[33].

Imaging probes for Magnetic Resonance Imaging (MRI)

MRI is a non-irradiant imaging technique performed in radiology, using pulses of radio waves that excite the nuclear spin energy transition, and magnetic field gradients localize the signal in space. The result is pictures of anatomy and physiological process with high spatial resolution and excellent soft tissue contrast but with limited sensitivity and quantification challenges (Figure 2). Compared to nuclear imaging, which can be performed using tracer dose of radioligands, the contrast agents used for MRI must be used at pharmacological doses. The variety of available compounds is also limited and predominantly relies on the use of metals (gadolinium for example), associated to a complex chemistry (Figures 2 & 3).

Gd-EOB-DTPA

Gd-EOB-DTPA (gadolinium-ethoxybenzyl-diethylenetriamine-pentaacetic acid (Figure 3), also called gadoxetate, is a hepatobiliary MRI contrast agent based on the extracellular fluid marker gadopentetate (gadolinium-diethylenetriamine-pentaacetic

acid). The introduction of the lipophilic ethoxybenzyl moiety to gadopentetate resulted in liver-specific contrast enhancement due to specific uptake into hepatocytes and biliary excretion of Gd-EOB-DTPA[34]. The substance benefits from a suitable complex stability *in vivo*, without any apparent biotransformation[34].

An *in vitro* study performed with transporter expressing *Xenopus laevis* oocytes, demonstrated that Gd-EOB-DTPA is taken up by rodent Slco1a1 but not Slco1a2[34]. The Slco-mediated uptake was inhibited by bromosulfophtalein (BSP), rifamycin, rifampicin and was shown saturable using a high concentration of Gd-EOB-DTPA[34]. The uptake of Gd-EOB-DTPA, as well as ^{111}In-EOB-DTPA, was shown to correlate with Slco1a1 expression in cells[33]. An *in vitro* study using human embryonic kidneys 293 (HEK293) cells transfected with the human *SLCO* transporter genes showed that Gd-EOB-DTPA is substrate and inhibitor of SLCO1B1 and SLCO1B3 but not SLCO2B1[35] (Table 2). Gd-EOB-DTPA is a substrate of SLC10A1 (NTCP) which may also contribute to its liver uptake[35] (Figure 1). Gd-EOB-DTPA was shown to be substrate of ABCC2[36], which impact on biliary secretion has been confirmed *in vivo* in Mrp2-deficient rats[36] (Table 2). Gd-EOB-DTPA is also an *in vitro* substrate of SLCO1A2 and ABCC3 (MRP3) but not the apical sodium-dependent bile acid transporter (ABST, SLC10A2) and organic cation transporter 3 (SLC22A3)[36].

A decrease in Slco1a1 protein expression in congestive rat livers was shown to be correlated with a reduced signal intensity of Gd-EOB-DTPA observed in a rat model of liver congestion[37]. Lagadec and coworkers recently reported a correlation between the hepatic extraction fraction of Gd-EOB-DTPA and the expression of Slco1a1 in a rat model of advanced liver fibrosis[38].

In humans, *in vitro* to *in vivo* correlation has been verified by a retrospective study in patients with hepatocellular carcinoma (HCC). Gd-EOB-DTPA MR data were compared to SLCO expression in resected hypervascular HCC. A correlation has been found between positive expression of SLCO1B1 and/or SLCO1B3 in pathologic liver cells and a significantly higher signal enhancement due to Gd-EOB-DTPA administration[39].

BOPTA

BOPTA (gadolinium benzyl-oxypropionictetraacetate; Figure 3) is another MRI contrast agent labeled with gadolinium. *In situ* perfusion of rat livers has shown that BOPTA uptake was completely inhibited by BSP, thus suggesting that the sinusoidal uptake of BOPTA may involve Slco-mediated transport[40]. The identification of isoforms responsible for BOPTA hepatic uptake was performed *in vitro* in *Xenopus laevis* oocytes: BOPTA was predominantly transported by rodent Slco1a1, Slco1a2 and Slco1b2[40]. Abcc2 was shown to mediate the bile excretion of BOPTA in rats, thus highlighting that the function of both sinusoidal and canalicular transporters is important to determine the liver kinetics of BOPTA[40] (Table 2).

Imaging probes for Positron Emission Tomography (PET)

PET is another nuclear imaging modality using β^+-emitting isotopes. Thanks to a high sensitivity of PET scanners, radiopharmaceutical agents used for PET imaging can be administered at tracer dose. The advantages of PET over SPECT include higher sensitivity (detection efficiency), better temporal and spatial resolution, at least in humans and large animals. PET imaging benefits from straightforward 3D quantifiable recordings (Figure 2). The β^+ emitter most routinely used in clinic is fluorine-18 (^{18}F, $T_{1/2}$ = 109.8 minutes), whereas carbon-11 (^{11}C, $T_{1/2}$ = 20.3 minutes) is frequently used

in research. Because of their short half-lives, radiotracers involving such β^+ emitters must be synthetized, controlled and administered quickly after the production of the radionuclide, mainly obtained from a cyclotron. Compared to isotopes used for SPECT and MR imaging contrast agents, β^+-emitting radionuclides offer the possibility to radiolabel a wider range of molecules[19]. PET imaging using radiolabeled analogs of drugs is increasingly used to elucidate the importance of transporters for tissue distribution[19,41]. PET imaging cannot distinguish the tissue radioactivity associated with the parent radiotracer or its radiometabolites that carry the radiolabeled isotopes. The presence of radiometabolites has thus to be taken into account for accurate estimation of transporter function *in vivo*[42].

(15*R*)-^{11}C-TIC-Me

(15*R*)-^{11}C-TIC-Me ((15*R*)-16-*m*-tolyl-17,18,19,20-tetranorisocarbacyclin methyl ester; Figure 2) was originally developed for PET of prostacyclin receptors in the central nervous system (Figure 3). (15*R*)-^{11}C-TIC-Me is a pro-drug and is rapidly hydrolyzed *in vivo* in its acid active form, the (15*R*)-^{11}C-TIC, subjected to hepatic clearance[20,21]. An *in vitro* study evidenced a significant and saturable increase in the accumulation of (15*R*)-^{11}C-TIC in SLCO1B1 and SLCO1B3-expressing cells compared to HEK293 control and SLCO2B1-expressing cells[21]. Both transporters were involved in hepatic uptake of (15*R*)-^{11}C-TIC with a larger contribution of SLCO1B1 compared to SLCO1B3 (69.3% *versus* 30.7%)[43]. In rats, (15*R*)-^{11}C-TIC is primarily excreted by the liver and, to a lesser extent, by the kidneys[20]. This hepatic transport was investigated in humans by Takashima and coworkers using (15*R*)-^{11}C-TIC-Me PET imaging. Healthy volunteers underwent dynamic (15*R*)-^{11}C-TIC-Me PET scanning before and one hour after oral administration of rifampicin (600 mg)[21]. Liver uptake and clearance of radioactivity were decreased in subjects pretreated with rifampicin, suggesting that

(15*R*)-^{11}C-TIC is substrate of both the uptake (SLCO) and biliary efflux (ABCC2) transporters *in vivo* (Figure 4). This study provided a convincing proof on the dramatic role of SLCO function in controlling the liver uptake of its substrates in humans (Table 2). However, several radiometabolites have been detected in human plasma, cultured hepatocytes as well as in blood, bile and liver of rats[20,21]. Alternative radioligands with improved metabolic stability are therefore required for accurate quantification of SLCO-function *in vivo*.

^{11}C-SC-62807

SC-62807 is the main metabolite of celecoxib, a selective COX-2 inhibitor. The liver metabolism of celecoxib involves two sequential oxidative pathways, initially to a hydroxymethyl metabolite (SC-60613) and upon subsequent further oxidation to a carboxylic acid metabolite (SC-62807). The majority of celecoxib is excreted into the bile as SC-62807[44–46]. Therefore, ^{11}C-celecoxib is not suitable for PET imaging because of its extensive metabolism. Intravenously administered ^{11}C-SC-62807 (Figure 3) is rapidly eliminated in mice and rats *via* hepatobiliary and renal excretion without further metabolism[44,47]. This metabolic stability makes the ^{11}C-SC-62807 an attractive PET tracer. The uptake of ^{11}C-SC-62807 was shown to be increased in HEK293 cells expressing SLCO1B1 and SLCO1B3 compared to parent cells[47]. ^{11}C-SC-62807 is known to be a substrate of the efflux transporter ABCG2 (Breast cancer resistance protein, BCRP), expressed at the liver-bile interface in Human[44,47] (Figure 1).

^{11}C-telmisartan

Telmisartan is a non-peptide selective angiotensin II type 1 receptor antagonist, broadly used as an antihypertensive drug[48]. Telmisartan is converted in the liver into

its pharmacologically inactive acylglucuronide (telmisartan-O-acyl-glucuronide) by UDP-glucuronyl-transferase, which is rapidly excreted in the intestine through the hepatobiliary system[49,50]. *In vitro* studies have shown that telmisartan and telmisartan-O-acyl-glucuronide are predominantly transported by the human SLCO1B3, rather than SLCO1B1[51,52]. Telmisartan-O-acyl-glucuronide is a substrate of ABCB1 (P-glycoprotein, P-gp), ABCG2 (BCRP) and ABCC2 (MRP2) expressed at the liver bile-interface[51–53] (Figure 1).

In rats, the co-administration of rifampicin decreased the amount of radioactivity in the liver and intestine, thus confirming the importance of Slco for ^{11}C-telmisartan (Figure 3) liver uptake[49]. ^{11}C-telmisartan has already been administered in humans for a biodistribution and radiation dosimetry study[50] (Table 2). To our knowledge, no clinical SLCO inhibition studies has been reported for this radiotracer yet.

^{11}C-dehydropravastatin

Statins are currently used to treat cholesterol and dyslipidemia. Their excretion *via* hepatobiliary route and known transport by different SLCO isoforms make statins interesting radiotracer candidates for the study of SLCO transport function *in vivo*.

The first radiolabeled statin used for PET was a pravastatin derivative, the ^{11}C-dehydropravastatin[54] (Figure 3). *In vitro,* dehydropravastatin was shown to accumulate in freshly isolated rat hepatocytes and rifampicin, a potent Slco inhibitor, dose dependently inhibited this uptake[54]. This result was confirmed *in vivo* in rats using ^{11}C-dehydropravastatin PET imaging, showing that both the accumulation of radioactivity in the liver and its excretion into the bile, were decreased after injection of rifampicin[55]. This study also confirmed that Abcc2 controls the biliary efflux of ^{11}C-dehydropravastatin[55]. At least one identifiable metabolite and other metabolites of ^{11}C-

dehydropravastatin were observed in plasma. Several radiometabolites could be detected in the liver and the bile, so that accurate quantification of transporter function remained difficult[55].

^{11}C-rosuvastatin

Rosuvastatin is a hydrophilic statin that provides the advantage over the previous statin to be a market approved drug, thus facilitating its acceptance as a PET probe in humans. The hepatic transport of rosuvastatin has been widely studied and it was shown to be a substrate *in vitro* of SLCO1B1 and SLCO1B3, with a predominant contribution of SLCO1B1[56,57]. Among SLCO transporters, rosuvastatin is also transported by SLCO2B1 and SLCO1A2[56–58]. Rosuvastatin is also a substrate of SLC10A1 (NTCP), ABCC2 (MRP2) and ABCG2 (BCRP)[56–58]. ^{11}C-rosuvastatin (Figure 3) has been studied in control rats *versus* Slco-inhibited rats using rifampicin. The hepatic distribution was significantly reduced in rats pretreated with rifampicin[59]. A decrease in the distribution of ^{11}C-rosuvastatin in the kidneys was also reported, suggesting a role for extrahepatic Slco function[59]. ^{11}C-rosuvastatin was shown to be metabolized in rat over the 90 minutes scanning and rifampicin inhibited the formation of metabolites[59].

^{18}F-pitavastatin

^{18}F-pitavastatin (Figure 3) is selectively taken up into the liver mainly *via* SLCO1B1[60]. For now, it is the only fluorine-containing pharmaceutical agent for imaging SLCO. Pitavastatin is a substrate of multiple hepatocyte transporters including the human SLCO1B1, SLCO1B3, SLCO1A2, SLC22A8 (OAT3), SLC10A1 (NTCP) and the rodent Slco1a1 and Slco1b2[61]. Because of radiosynthesis issues, a new derivative, ^{18}F-PTV-F1 was recently developed, in which a ^{18}F-fluoroethoxy group is substituted for the ^{18}F-

fluoro group of ^{18}F-pitavastatin[62,63]. This new derivative was shown to be transported *in vitro* by both SLCO1B1 and SLCO1B3 as a substrate, and its relative transport activities by the transporters were almost similar to those of pitavastatin[63]. No troublesome metabolites could be detected for neither pitavastatin nor with PTV-F1 after 10 minutes incubation in human liver microsomes[63].

^{11}C-glyburide

Glyburide, also called glibenclamide, a hypoglycemic agent from the sulfonylurea class, is commonly used in the treatment of noninsulin-dependent diabetes. This drug is substrate of many transporters, including SLCO isoforms. *In vitro* studies indicated that glyburide is preferentially transported by SLCO2B1[64], SLCO1A2 and to a lesser extent, SLCO1B1[65]. Glyburide is a substrate for transporters of the ABC superfamily, expressed in hepatocytes, including ABCB1, ABCG2, ABCC1 and ABCC3[66–71] (Figure 1). A preclinical study in baboons was carried out with ^{11}C-glyburide (Figure 5), the radiolabeled analogue of glyburide[71]. The primates were pretreated either by rifampicin, the SLCO inhibitor, or by cyclosporin A, a dual P-gp and SLCO inhibitor. An increase of radioactivity was observed in the plasma of treated baboons associated to a decrease of radioactivity in the liver parenchyma. The particularity of this study in non-human primates was the ability to explore other organs such as the renal cortex, brain, myocardium, pancreas and lungs. In the kidneys, the tissue/plasma ratio of ^{11}C-glyburide was reduced in the renal cortex of SLCO-inhibited baboons. The impact of renal SLCO function to urinary clearance and exposure to the kidney remains to be assessed. Both rifampicin and cyclosporin A similarly inhibited the uptake of the radiotracer into the myocardium, suggesting SLCO2B1 would mediate its cardiac uptake since SLCO1B1 and SLCO1A2 are not expressed in this tissue[18,72]. No relevant influence of SLCO inhibition was found in lungs, pancreas and brain[71]. Glyburide was

slowly metabolized with 70% of parent ^{11}C-glyburide in the plasma after 60 min scanning. Interestingly, no radiometabolites could be detected after cyclosporin A or rifampicin pretreatment[71]. This observation illustrates the interplay between transporter-mediated liver uptake and metabolic enzymes in controlling the liver metabolism of drugs. ^{11}C-glyburide appears to be a promising SLCO PET tracer to study SLCO2B1-mediated transport in extrahepatic organs *in vivo*.

Conclusion and perspectives

Molecular imaging aims at developing new compounds dedicated to the study of a specific molecular target. Interestingly, current probes for SLCO-imaging have often been used for decades to study hepatobiliary function in patients (^{99m}Tc-mebrofenin SPECT imaging, Gd-EOB-DTPA MRI). The importance of SLCO-mediated transport on their hepatic uptake was discovered many years after, thus providing a molecular determinant for their predominant liver accumulation[73]. The main advantage of the use of radiopharmaceutical and contrast agents for the study of SLCO transport function is their excellent availability and the possibility to perform clinical studies in most hospital radiology and/or nuclear medicine departments.

Recent PET imaging probes are derived from drugs which SLCO-mediated transport has been evidenced once the importance of SLCO for PK has been highlighted, several years after their initial acceptance for clinical use on the market. The main advantage of PET over SPECT and MRI is the chemical diversity of the possible compounds to label (Figure 2 & 3), which compensates for the poor availability of the radiopharmaceutical preparations that is still limited to PET research centers. Medicinal chemistry and the development of radiolabeling methods may contribute to

the development of innovative SLCO probes for PET, with improved specificity, metabolic stability and sensitivity to modulation of SLCO function.

Indeed, the presence of several SLCO isoforms in the liver and other organs suggests a differential impact and regulation of their function *in vivo*. So far, only few SLCO-imaging probes have proven to be specific over a single SLCO isoform. It is possible to estimate a global SLCO-transport function but it remains difficult to characterize the interplay between SLCO isoforms in controlling the tissue uptake of their common substrates[11].

Another possibility to gain specificity regarding SLCO isoforms would be the use of isoform-specific SLCO inhibitors. This strategy would be useful to highlight the respective contribution of each transport *in vivo*. Unfortunately, most safe SLCO inhibitors for clinical use (rifampicin, cyclosporin) are broad spectrum SLCO inhibitors. Specificity data can be obtained in mice, using transporter deficient animals. However, clinical extrapolation has proven to be difficult for the study of SLCO function. So far, specificity of SLCO-imaging probes over different SLCO isoforms is assessed *in vitro* only, using human protein expressing systems. The development of isoform-specific inhibitors of SLCO function would be an important step forward for the clinical validation of the probes, in order to assess their *in vivo* specificity.

It is noteworthy that imaging SLCO function offers the possibility to use different imaging modalities, including SPECT, PET and MRI. Multi-modality imaging is increasingly regarded as an innovative approach to make the best of each individual modality. Combination of imaging modalities has been successfully performed to detect Slco1a1 overexpression using ^{111}In-EOB-DTPA and Gd-EOB-DTPA as probes, thus benefiting from the high sensitivity of nuclear imaging and the excellent spatial

resolution of MRI[33]. In this framework, the development of multimodal probes, that can be simultaneously detected and/or quantified using hybrid PET/MR systems, may offer new opportunities to study SLCO function *in vivo*. Indeed, such a multimodal imaging system may allow for increased time and spatial resolution with improved detection sensitivity using a single scan and a single tracer administration in animals or humans. This strategy would be useful to make sure the system of interest is probed in the exact same pathophysiological state with the two imaging modalities[74].

Acknowledgments

This work was funded by a grant from ANR-16-CE17-0011-001.

References

1. Giacomini KM, Huang S-M, Tweedie DJ, Benet LZ, Brouwer KLR, et al 2010 Membrane transporters in drug development. Nat Rev Drug Discov. 9(3):215–236.

2. König J, Müller F, Fromm M 2013 Transporters and drug-drug interactions: important determinants of drug disposition and effects. Pharmacol Rev. 65(3):944–966.

3. Zamek-Gliszczynski MJ, Hoffmaster KA, Tweedie DJ, Giacomini KM, Hillgren KM 2012 Highlights from the International Transporter Consortium second workshop. Clin Pharmacol Ther 92(5):553–556.

4. Kusuhara H 2013 Imaging in the study of membrane transporters. Clin Pharmacol Ther 94(1):33–36.

5. Muzi M, Mankoff DA, Link JM, Shoner S, Collier AC, et al 2009 Imaging of cyclosporine inhibition of P-glycoprotein activity using 11C-verapamil in the brain: studies of healthy humans. J Nucl Med 50(8):1267–1275.

6. Kreisl WC, Liow J-S, Kimura N, Seneca N, Zoghbi SS, et al 2010 P-glycoprotein function at the blood-brain barrier in humans can be quantified with the substrate radiotracer 11C-N-desmethyl-loperamide. J Nucl Med 51(4):559–566.

7. Pottier G, Marie S, Goutal S, Auvity S, Peyronneau M-A, et al 2016 Imaging the impact of the P-glycoprotein (Abcb1) function on the brain kinetics of metoclopramide. J Nucl Med 57(2):309–314.

8. Bauer M, Karch R, Tournier N, Cisternino S, Wadsak W, et al 2017 Assessment of P-glycoprotein transport activity at the human blood-retinal barrier with (R)-11C-verapamil PET. J Nucl Med 58(4) :678-681.

9. Kannan P, John C, Zoghbi SS, Halldin C, Gottesman MM, et al 2009 Imaging the function of P-glycoprotein with radiotracers: pharmacokinetics and in vivo applications. Clin Pharmacol Ther 86(4):368–377.

10. Hagenbuch B, Stieger B 2013 The SLCO (former SCL21) superfamily of transporters. Mol Aspects Med 34(2–3):396-412.

11. Stieger B, Hagenbuch B 2014 Organic anion-transporting polypeptides. Curr Top Membr 73:205–232.

12. Roth M, Obaidat A, Hagenbuch B 2012 OATPs, OATs and OCTs: the organic anion and cation transporters of the SLCO and SCL22A gene superfamilies. Br J Pharmacol 165(5):1260–1287.

13. Obaidat A, Roth M, Hagenbuch B 2012 The expression and function of Organic Anion Transporting Polypeptides in normal tissues and in cancer. Annu Rev Pharmacol Toxicol 52:135-151.

14. Hagenbuch B, Gui C 2008 Xenobiotic transporters of the human organic anion transporting polypeptides (OATP) family. Xenobiotica 38(7–8):778–801.

15. Kalliokoski A, Niemi M 2009 Impact of OATP transporters on pharmacokinetics. Br J Pharmacol 158(3):693–705.

16. Shitara Y, Maeda K, Ikejiri K, Yoshida K, Horie T, Sugiyama Y 2013 Clinical significance of organic anion transporting polypeptides (OATPs) in drug disposition: their roles in hepatic clearance and intestinal absorption. Biopharm Drug Dispos 34(1):45–78.

17. Chu X, Bleasby K, Evers R 2013 Species differences in drug transporters and implications for translating preclinical findings to humans. Expert Opin Drug Metab Toxicol 9(3):237–52

18. Nishimura M, Naito S 2008 Tissue-specific mRNA expression profiles of human solute carrier transporter superfamilies. Drug Metab Pharmacokinet 23(1):22–44.

19. Mann A, Semenenko I, Meir M, Eyal S 2015 Molecular imaging of membrane transporters' activity in cancer: a picture is worth a thousand tubes. The AAPS J 17(4):788-801.

20. Takashima T, Nagata H, Nakae T, Cui Y, Wada Y, et al 2010 Positron emission tomography studies using (15R)-16-m-[11C]tolyl-17,18,19,20-tetranorisocarbacyclin methyl ester for the evaluation of hepatobiliary transport. J Pharmacol Exp Ther 335(2):314–323.

21. Takashima T, Kitamura S, Wada Y, Tanaka M, Shigihara Y, et al 2012 PET imaging–based evaluation of hepatobiliary transport in humans with (15R)-11C-TIC-Me. J Nucl Med 53(5):741–748.

22. Tournier N, André P, Blondeel S, Rizzo-Padoin N, du Moulinet d'Hardemarre A, et al 2009 Ibogaine labeling with 99mTc-tricarbonyl: synthesis and transport at the mouse blood-brain barrier. J Pharm Sci 98(12):4650–4660.

23. Bailey DL, Willowson KP 2013 An evidence-based review of quantitative SPECT imaging and potential clinical applications. J Nucl Med 54(1):83–89.

24. Ghibellini G, Leslie E, Pollack G, Brouwer K 2008 Use of Tc-99m mebrofenin as a clinical probe to assess altered hepatobiliary transport: integration of in vitro, pharmacokinetic modeling, and simulation studies. Pharm Res 25(8):1851-1860.

25. de Graaf W, Häusler S, Heger M, van Ginhoven T, van Cappellen G, et al 2011 Transporters involved in the hepatic uptake of 99mTc-mebrofenin and indocyanine green. J Hepatol 54(4):738–745.

26. Neyt S, Huisman M, Vanhove C, Man H, Vliegen M, et al 2013 In vivo visualization and quantification of (disturbed) Oatp-mediated hepatic uptake and Mrp2-mediated biliary excretion of 99mTc-mebrofenin in mice. J Nucl Med 54(4):624–630.

27. Swift B, Yue W, Brouwer KLR 2010 Evaluation of (99m)technetium-mebrofenin and (99m)technetium-sestamibi as specific probes for hepatic transport protein function in rat and human hepatocytes. Pharm Res 27(9):1987–1998.

28. Bonnaventure P, Pastor CM 2014 Quantification of drug transport function across the multiple resistance-associated protein 2 (Mrp2) in rat livers. Int J Mol Sci 16(1):135–147.

29. Kato-Azuma M 1982 Tc-99m(Sn)-N-pyridoxylaminates: a new series of hepatobiliary imaging agents. J Nucl Med 23(6):517–524.

30. Narabayashi I, Hamada T, Aoki O, Suematsu T 1987 Small hepatocellular carcinoma visualized with technetium-99m(Sn)-N-pyridoxyl-5-methyltryptophan. Ann Nucl Med 1(1):39–42.

31. Narabayashi I, Sugimura K, Ishido N, Kajita A 1987 Quantitative analysis by digital computer of 99mTc-N-pyridoxyl-5-methyltryptophan (99mTc-PMT) hepatogram in diffuse parenchymal liver diseases. Eur J Nucl Med 13(6):285–287.

32. Kobayashi M, Nakanishi T, Nishi K, Higaki Y, Okudaira H, et al 2014 Transport mechanisms of hepatic uptake and bile excretion in clinical hepatobiliary scintigraphy with 99mTc-N-pyridoxyl-5-methyltryptophan. Nucl Med Biol 41(4):338–42.

33. Stephen Patrick P, Hammersley J, Loizou M, Kettunen M, Rodrigues T, et al 2014 Dual-modality gene reporter for in vivo imaging. Proc Natl Acad Sci U S A 111(1):415-420.

34. van Montfoort J, Stieger B, Meijer D, Weinmann H, Meier P, Fattinger K 1999 Hepatic uptake of the magnetic resonance imaging contrast agent gadoxetate by the Organic Anion Transporting Polypeptide Oatp1. J Pharmacol Exp Ther 290(1):153–157.

35. Leonhardt M, Keiser M, Oswald S, Kühn J, Jia J, et al 2010 Hepatic uptake of the magnetic resonance imaging contrast agent Gd-EOB-DTPA: role of human organic anion transporters. Drug Metab Dispos 38(7):1024–1028.

36. Jia J, Puls D, Oswald S, Jedlitschky G, Kühn JP, et al 2014 Characterization of the intestinal and hepatic uptake/efflux transport of the magnetic resonance imaging contrast agent gadolinium-ethoxylbenzyl-diethylenetriamine-pentaacetic acid. Invest Radiol 49(2):78–86.

37. Shimizu A, Kobayashi A, Motoyama H, Sakai H, Yamada A, et al 2015 Features of acute liver congestion on gadoxetate disodium-enhanced MRI in a rat model: role of organic anion-transporting polypeptide 1a1. J. Magn Reson Imaging 42(3):828–836.

38. Lagadec M, Doblas S, Giraudeau C, Ronot M, Lambert SA, et al 2015 Advanced fibrosis: correlation between pharmacokinetic parameters at dynamic gadoxetate-enhanced MR imaging and hepatocyte organic anion transporter expression in rat liver. Radiology 274(2):379–386.

39. Tsuboyama T, Onishi H, Kim T, Akita H, Hori M, et al 2010 Hepatocellular carcinoma: hepatocyte-selective enhancement at gadoxetic acid–enhanced MR imaging—correlation with expression of sinusoidal and canalicular transporters and bile accumulation. Radiology 255(3):824–833.

40. Planchamp C, Hadengue A, Stieger B, Bourquin J, Vonlaufen A, et al 2007 Function of both sinusoidal and canalicular transporters controls the concentration of organic anions within hepatocytes. Mol Pharmacol 71(4):1089–97.

41. Tournier N, Goutal S, Auvity S, Traxl A, Mairinger S, et al 2017 Strategies to inhibit ABCB1- and ABCG2-mediated efflux transport of erlotinib at the blood-brain barrier: a PET study in non-human primates. J Nucl Med 58(1):117-122.

42. Pike VW 2009 Pet radiotracers: crossing the blood-brain barrier and surviving metabolism. Trends Pharmacol Sci 30(8):431–440.

43. Testa A, Zanda M, Elmore C, Sharma P 2015 PET tracers to study clinically relevant hepatic transporters. Mol Pharmaceutics 12(7):2203–2216.

44. Takashima-Hirano M, Takashima T, Katayama Y, Wada Y, Sugiyama Y, et al 2011 Efficient sequential synthesis of PET probes of the COX-2 inhibitor [11C]celecoxib and its major metabolite [11C]SC-62807 and in vivo PET evaluation. Bioorg Med Chem 19(9):2997–3004.

45. Paulson S, Zhang J, Breau A, Hribar J, Liu N, et al 2000 Pharmacokinetics, tissue distribution, metabolism, and excretion of celecoxib in rats. Drug Metab Dispos 28(5):514–521.

46. Paulson SK, Hribar J, Liu N, Hajdu E, Bible R, et al 2000 Metabolism and excretion of [14C]celecoxib in healthy male volunteers. Drug Metab Dispos 28(3):308–314.

47. Takashima T, Wu C, Takashima-Hirano M, Katayama Y, Wada Y, et al 2013 Evaluation of breast cancer resistance protein function in hepatobiliary and renal excretion using pet with 11C-SC-62807. J Nucl Med 54(2):267–276.

48. Iimori H, Hashizume Y, Sasaki M, Kajiwara Y, Sugimoto Y, et al 2011 First automatic radiosynthesis of 11C labeled telmisartan using a multipurpose synthesizer for clinical research use. Ann Nucl Med 25(5):333–337.

49. Takashima T, Hashizume Y, Katayama Y, Murai M, Wada Y, et al 2011 The involvement of organic anion transporting polypeptide in the hepatic uptake of telmisartan in rats: PET studies with [11C]telmisartan. Mol Pharmaceutics 8(5):1789–1798.

50. Shimizu K, Takashima T, Yamane T, Sasaki M, Kageyama H, et al 2012 Whole-body distribution and radiation dosimetry of [11C]telmisartan as a biomarker for hepatic organic anion transporting polypeptide (OATP) 1b3. Nucl Med Biol 39(6):847–853.

51. Ishiguro N, Maeda K, Kishimoto W, Saito A, Harada A, et al 2006 Predominant contribution of OATP1B3 to the hepatic uptake of telmisartan, an angiotensin II receptor antagonist, in humans. Drug Metab Dispos 34(7):1109–1115.

52. Ishiguro N, Maeda K, Saito A, Kishimoto W, Matsushima S, et al 2008 Establishment of a set of double transfectants coexpressing organic anion transporting polypeptide 1B3 and hepatic efflux transporters for the characterization of the hepatobiliary transport of telmisartan acylglucuronide. Drug Metab Dispos 36(4):796–805.

53. Nishino A, Kato Y, Igarashi T, Sugiyama Y 2000 Both cMOAT/MRP2 and another unknown transporter(s) are responsible for the biliary excretion of glucuronide conjugate of the nonpeptide angiotensinII antagonist, telmisaltan. Drug Metab. Dispos 28(10):1146–1148.

54. Shingaki T, Takashima T, Ijuin R, Zhang X, Onoue T, et al 2013 Evaluation of Oatp and Mrp2 activities in hepatobiliary excretion using newly developed positron emission tomography tracer [11C]dehydropravastatin in rats. J Pharmacol Exp Ther 347(1):193–202.

55. Ijuin R, Takashima T, Watanabe Y, Sugiyama Y, Suzuki M 2012 Synthesis of [11C]dehydropravastatin, a PET probe potentially useful for studying Oatp1b1 and Mrp2 transporters in the liver. Bioorg Med Chem. 20(12):3703–3709.

56. Kitamura S, Maeda K, Wang Y, Sugiyama Y 2008 Involvement of multiple transporters in the hepatobiliary transport of rosuvastatin. Drug Metab Dispos 36(10):2014–2023.

57. Ho R, Tirona R, Leake B, Glaeser H, Lee W, et al 2006 Drug and bile acid transporters in rosuvastatin hepatic uptake: function, expression, and pharmacogenetics. Gastroenterology 130(6):1793–1806.

58. Hobbs M, Parker C, Birch H, Kenworthy K 2012 Understanding the interplay of drug transporters involved in the disposition of rosuvastatin in the isolated perfused rat liver using a physiologically-based pharmacokinetic model. Xenobiotica 42(4):327–338.

59. He J, Yu Y, Prasad B, Link J, Miyaoka R, et al 2014 Pet imaging of Oatp-mediated hepatobiliary transport of [11C]rosuvastatin in the rat. Mol Pharmaceutics 11(8):2745–2754.

60. Hirano M, Maeda K, Shitara Y, Sugiyama Y 2004 Contribution of OATP2 (OATP1B1) and OATP8 (OATP1B3) to the hepatic uptake of pitavastatin in humans. J Pharmacol Exp Ther 311(1):139–146.

61. Fujino H, Saito T, Ogawa S-I, Kojima J 2005 Transporter-mediated influx and efflux mechanisms of pitavastatin, a new inhibitor of HMG-CoA reductase. J Pharm Pharmacol 57(10):1305–1311.

62. Yagi Y, Kimura H, Arimitsu K, Ono M, Maeda K, et al 2015 The synthesis of [18F]pitavastatin as a tracer for hOATP using the Suzuki coupling. Org Biomol Chem 13(4):1113–1121.

63. Kimura H, Yagi Y, Arimitsu K, Maeda K, Ikejiri K, et al 2016 Radiosynthesis of novel pitavastatin derivative ([18F]PTV-F1) as a tracer for hepatic OATP using a one-pot synthetic procedure. J Label Compd Radiopharm 59(13):565–575.

64. Satoh H, Yamashita F, Tsujimoto M, Murakami H, Koyabu N, et al 2005 Citrus juices inhibit the function of human organic anion-transporting polypeptide OATP-B. Drug Metab Dispos 33(4):518–523.

65. Koenen A, Köck K, Keiser M, Siegmund W, Kroemer H, Grube M 2012 Steroid hormones specifically modify the activity of organic anion transporting polypeptides. Eur J Pharm Sci 47(4):774–780.

66. Gedeon C, Behravan J, Koren G, Piquette-Miller M 2006 Transport of glyburide by placental ABC transporters: implications in fetal drug exposure. Placenta 27(11–12):1096–1102.

67. Cygalova LH, Hofman J, Ceckova M, Staud F 2009 Transplacental pharmacokinetics of glyburide, rhodamine 123, and bodipy FL prazosin: effect of drug efflux transporters and lipid solubility. J Pharmacol Exp Ther 331(3):1118–1125.

68. Zhou L, Naraharisetti SB, Wang H, Unadkat JD, Hebert MF, Mao Q 2008 The breast cancer resistance protein (Bcrp1/Abcg2) limits fetal distribution of glyburide in the pregnant mouse: an obstetric-fetal pharmacology research unit network and university of washington specialized center of research study. Mol Pharmacol 73(3):949–959.

69. Pollex E, Lubetsky A, Koren G 2008 The role of placental breast cancer resistance protein in the efflux of glyburide across the human placenta. Placenta 29(8):743–747.

70. Hemauer SJ, Patrikeeva SL, Nanovskaya TN, Hankins GDV, Ahmed MS 2010 Role of human placental apical membrane transporters in the efflux of glyburide, rosiglitazone, and metformin. Am J Obstet Gynecol 202(4):383.e1-7.

71. Tournier N, Saba W, Cisternino S, Peyronneau M, Damont A, et al 2013 Effects of selected OATP and/or ABC transporter inhibitors on the brain and whole-body distribution of glyburide. AAPS J 15(4):1082–1090.

72. Grube M, Köck K, Oswald S, Draber K, Meissner K, et al 2006 Organic anion transporting polypeptide 2b1 is a high-affinity transporter for atorvastatin and is expressed in the human heart. Clin Pharmacol Ther 80(6):607–620.

73. Stieger B, Unadkat JD, Prasad B, Langer O, Gali H 2014 Role of (drug) transporters in imaging in health and disease. Drug Metab Dispos 42(12):2007–2015.

74. Louie A 2010 Multimodality imaging probes: design and challenges. Chem Rev 110(5):3146–3195.

Figure legends

Figure 1. Membrane transporters of importance for pharmacokinetics in hepatocytes. Transporters of the Solute Carrier (SLC) superfamily are shown as black circles. Transporters of the ATP-binding cassette (ABC) superfamily are shown as open circles. Transporters are named according to the HUGO nomenclature. Their most common aliases are mentioned between parentheses. Adapted from Zamek et al.[3]

Figure 2. Comparative performances of imaging modalities proposed to study SLCO function *in vivo*.

Figure 3. Chemical structures of probes used to study SLCO function *in vivo*

Figure 4. Color-coded PET images of abdominal region of healthy male subject after administration of (15R)-^{11}C-TIC-Me with and without rifampicin. Coronal maximum-intensity-projection PET images of radioactivity in abdominal region were captured at 5, 10, 15, 20, and 30 min after administration of (15R)-^{11}C-TIC-Me in absence (A) or presence (B) of 600 mg of rifampicin. This research was originally published in JNM. Tadayuki Takashima et al. J Nucl Med 2012;53:741-748 © by the Society of Nuclear Medicine and Molecular Imaging, Inc.[21]

Figure 5. ^{11}C-glyburide PET images obtained in the liver of baboons in baseline conditions and after Solute Carrier O (SLCO) inhibition. These are summed (0-10 min) PET images normalized by injected dose and animal weight (Standardized uptake value, SUV) in the absence (baseline) and the presence of SLCO inhibition (rifampicin). Corresponding experimental settings were originally reported by Tournier et al.[71]

Tables

Table 1. Human and rodent transporters of the Solute Carrier O (SLCO) family. The different SLCO transporters cluster into families (SLCO1-6) and subfamilies based on their amino acid sequence identities. Human genes and their corresponding protein and known aliases are reported in the left column. Corresponding rodent orthologues (gene, protein, aliases) are reported in the right column.[10] (Source: https://www.ncbi.nlm.nih.gov/gene/)

Table 2. Current imaging probes to study Solute Carrier O (SLCO) function.

Table 1

Human			Rodent		
Genes	**Proteins**	**Aliases**	**Genes**	**Proteins**	**Aliases**
SLCO1A2	SLCO1A2	SLC21A3, OATP-A	*Slco1a1*	Slco1a1	Slc21a1, Slc21a3, Oatp1
			Slco1a3	Slco1a3 (rat only)	Slco21a4, OAT-K1, OAT-K2, OAT-K3, OAT-K5, OAT-K6, OAT-K7; OAT-K8, OAT-K9, OAT-K11, OAT-K13, OAT-K14
			Slco1a4	Slco1a4	Slc21a5, Oatp2
			Slco1a5	Slco1a5	Slc21a7, Oatp3
			Slco1a6	Slco1a6	Slc21a13, Oatp5
SLCO1B1	SLCO1B1	SLC21A6, HBLR, LST-1, OATP2, OATP-C	*Slco1b2*	Slco1b2	Slc21a6, Slc21a10, Oatp4, lst-1
SLCO1B3	SLCO1B3	SLC21A8, LST-2, LST-3, HBLRR, , OATP8, LST-3TM13			
SLCO1C1	SLCO1C1	SLC21A14, OATP1, OATP-F, OATP14, OATP-RP5	*Slco1c1*	Slco1c1	Slc21a14, Oatp14, Oatpf, Bsat1
SLCO2A1	SLCO2A1	SLC21A2, PGT, MATR1, PHOAR2	*Slco2a1*	Slco2a1	Slc21a2, Pgt, Matr1
SLCO2B1	SLCO2B1	SLC21A9, OATP-B	*Slco2b1*	Slco2b1	Slc21a9, moat1
SLCO3A1	SLCO3A1	SLC21A11, OATP-D, OATP-RP3	*Slco3a1*	Slco3a1	Slc21a11, Anr1, MJAM
SLCO4A1	SLCO4A1	SLC21A12, OATP1, OATP-E, OATP-RP1, POAT	*Slco4a1*	Slco4a1	Slc21a12
SLCO4C1	SLCO4C1	SLC21A20, OATP-H, OATPX, OATP-M1, PRO2176	*Slco4c1*	Slco4c1	Slc21a20, Oatp-H, Oatp-M1, Oatp-R, PRO2176
SLCO5A1	SLCO5A1	SLCO21A15, OATP-J, OATP-RP4	*Slco5a1*	Slco5a1 (mouse only)	
SLCO6A1	SLCO6A1	OATP-I, OATPY, GST, CT48	*Slco6b1*	Slco6b1	Tst1, GST-1
			Slco6c1	Slco6c1	GST-2
			Slco6d1	Slco6d1	4921511I05Rik

Table 2

Imaging probes	SLCO-mediated transport *in vitro*	SLCO-mediated transport in animals	Clinical translation
^{99m}Tc-mebrofenin	SLCO1B1, SLCO1B3[24,26]	Studied in mice KO and after inhibition by rifampicin[26]	
^{99m}Tc-PMT	SLCO1B1, SLCO1B3[32]		
^{111}In-EOB-DTPA		Studied in mice transfected with a Slco1a1 xenograft[33]	
BOPTA	Slco1a1, Slco1a2, Slco1b2[40]		
Gd-EOB-DTPA	Slco1a1[34], SLCO1A2, SLCO1B1, SLCO1B3[35,36]	Studied in mice transfected with a Slco1a1 xenograft[33] and in liver congestive rats with decreased Slco1a1 expression[37,38]	Correlation with SLCO1B1 and SLCO1B3 expression in hepatocellular carcinoma nodules[39]
^{11}C-dehydropravastatin	Rifampicin inhibitable transport in isolated rat hepatocytes[54]	Studied in rats after inhibition by rifampicin[55]	
^{11}C-glyburide	SLCO1A2, SLCO1B1, SLCO2B1[64,65]	Studied in baboons after inhibition by rifampicin and cyclosporin[71]	
^{18}F-pitavastatin	SLCO1B1, SLCO1B3, SLCO1A2, Slco1a1, Slco1b2[61]		
^{18}F-PTV-F1	SLCO1B1, SLCO1B3[63]		
^{11}C-rosuvastatin	SLCO1B1, SLCO1B3, SLCO2B1, SLCO1A2[56–58]	Studied in rats after inhibition by rifampicin[59]	
^{11}C-SC-62807	SLCO1B1, SLCO1B3[47]		
^{11}C-telmisartan	SLCO1B3[51]	Studied in rats after inhibition by rifampicin[49]	Baseline biodistribution and radiation dosimetry[50]
(15*R*)-^{11}C -TIC-Me	SLCO1B1, SLCO1B3[21]		Inhibition study using rifampicin[21]

Figure 1

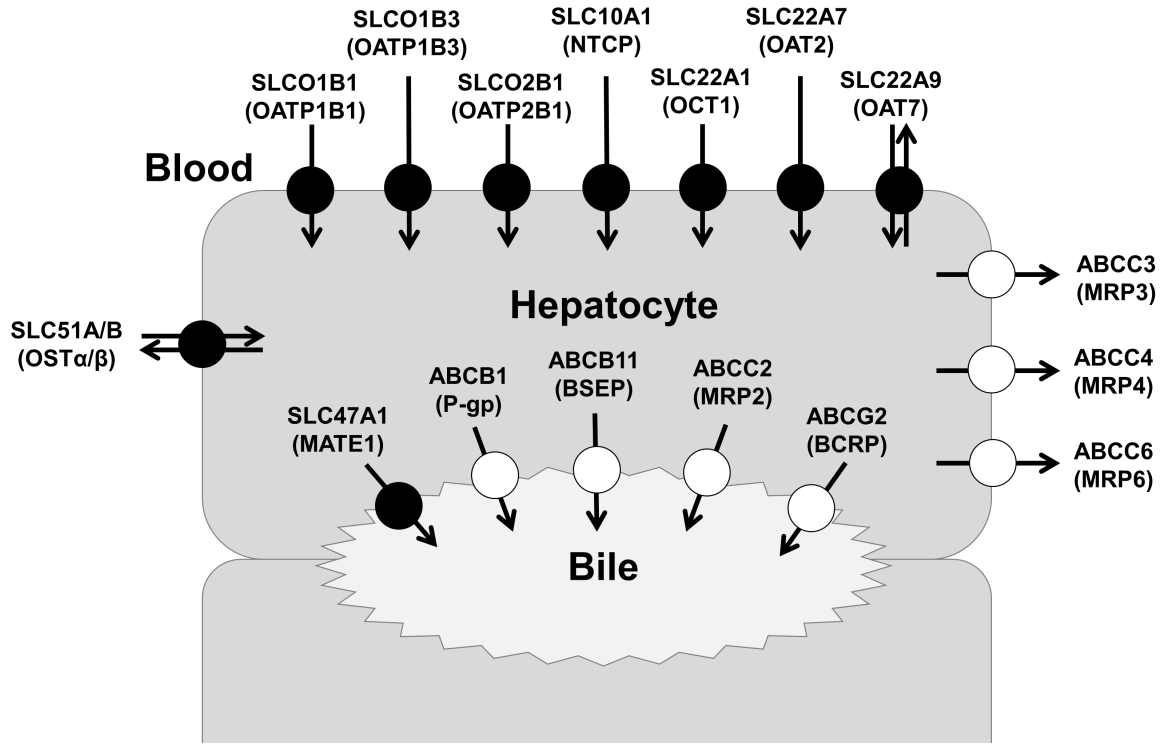
SLCO1B3
(OATP1B3)
SLC10A1
(NTCP)
SLC22A7
(OAT2)
SLCO1B1
(OATP1B1)
SLCO2B1
(OATP2B1)
SLC22A1
(OCT1)
SLC22A9
(OAT7)
Blood
ABCC3
(MRP3)
Hepatocyte
SLC51A/B
(OSTα/β)
ABCB1
(P-gp)
ABCB11
(BSEP)
ABCC2
(MRP2)
ABCC4
(MRP4)
SLC47A1
(MATE1)
ABCG2
(BCRP)
ABCC6
(MRP6)
Bile

Figure 2

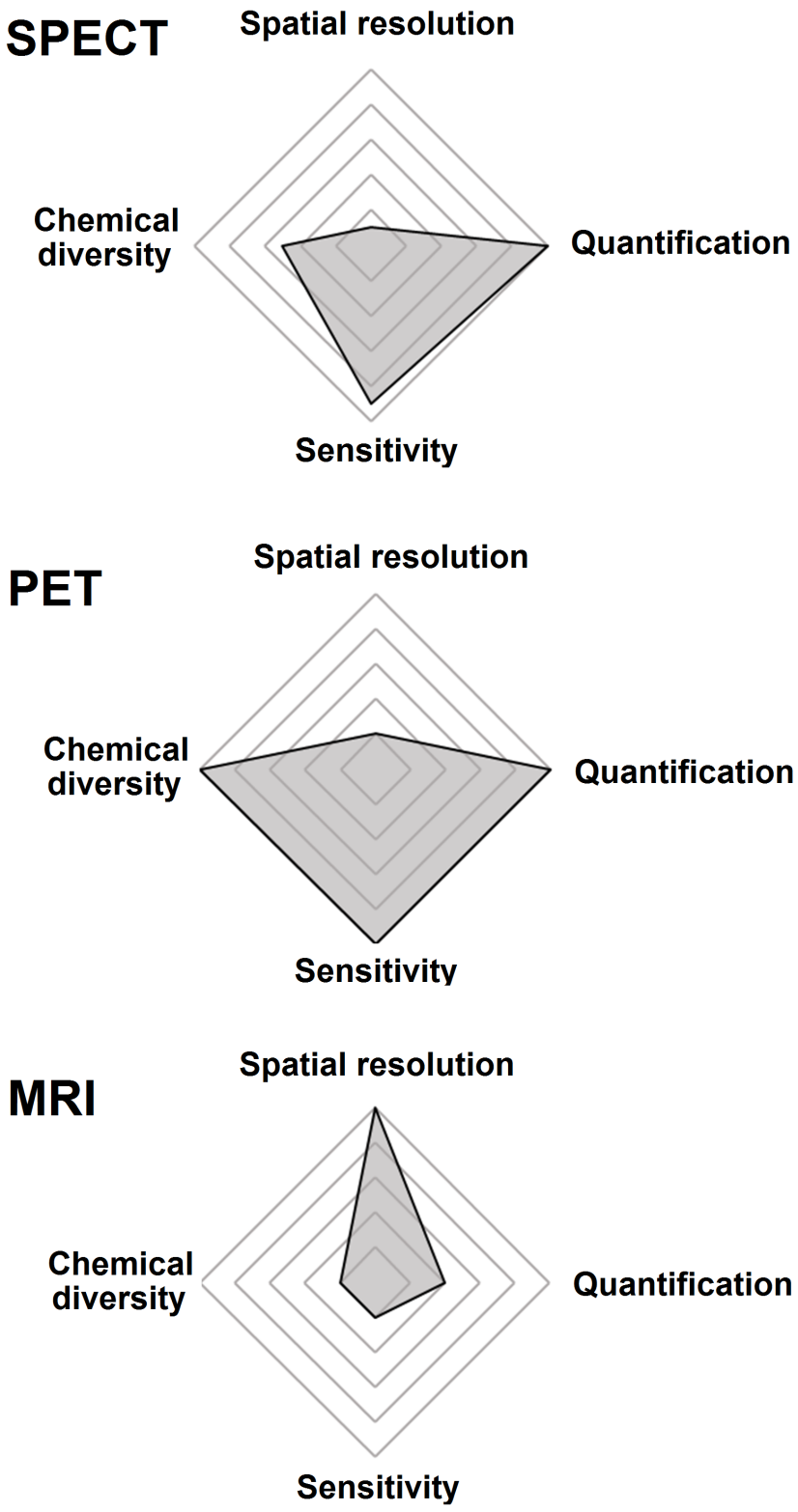
SPECT
Spatial resolution
Chemical diversity
Quantification
Sensitivity
PET
Spatial resolution
Chemical diversity
Quantification
Sensitivity
MRI
Spatial resolution
Chemical diversity
Quantification
Sensitivity

Figure 3

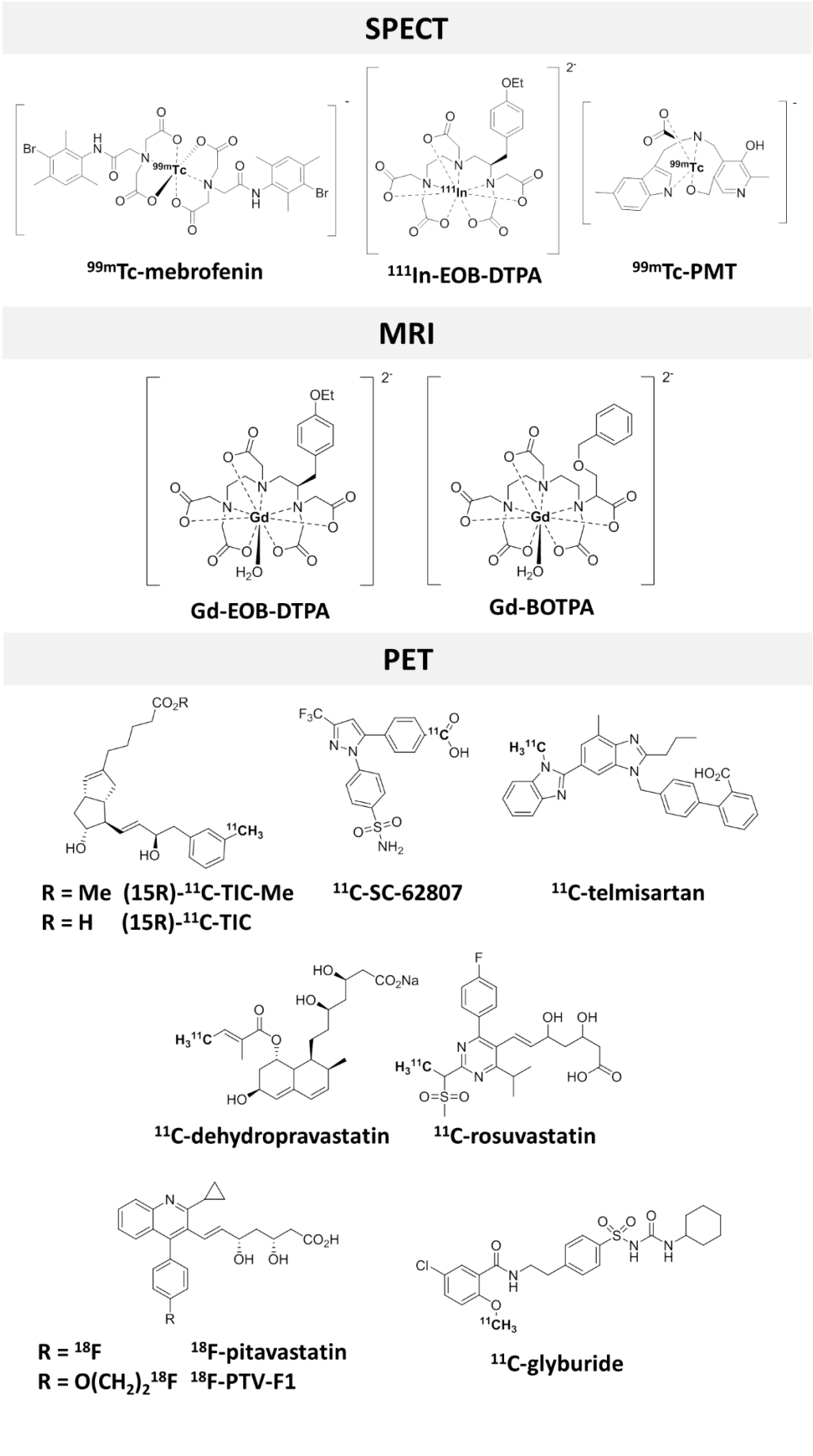
SPECT
99mTc-mebrofenin
111In-EOB-DTPA
99mTc-PMT
MRI
Gd-EOB-DTPA
Gd-BOTPA
PET
R = Me (15R)-11C-TIC-Me
R = H (15R)-11C-TIC
11C-SC-62807
11C-telmisartan
11C-dehydropravastatin
11C-rosuvastatin
R = 18F 18F-pitavastatin
R = O(CH2)218F 18F-PTV-F1
11C-glyburide

Figure 4

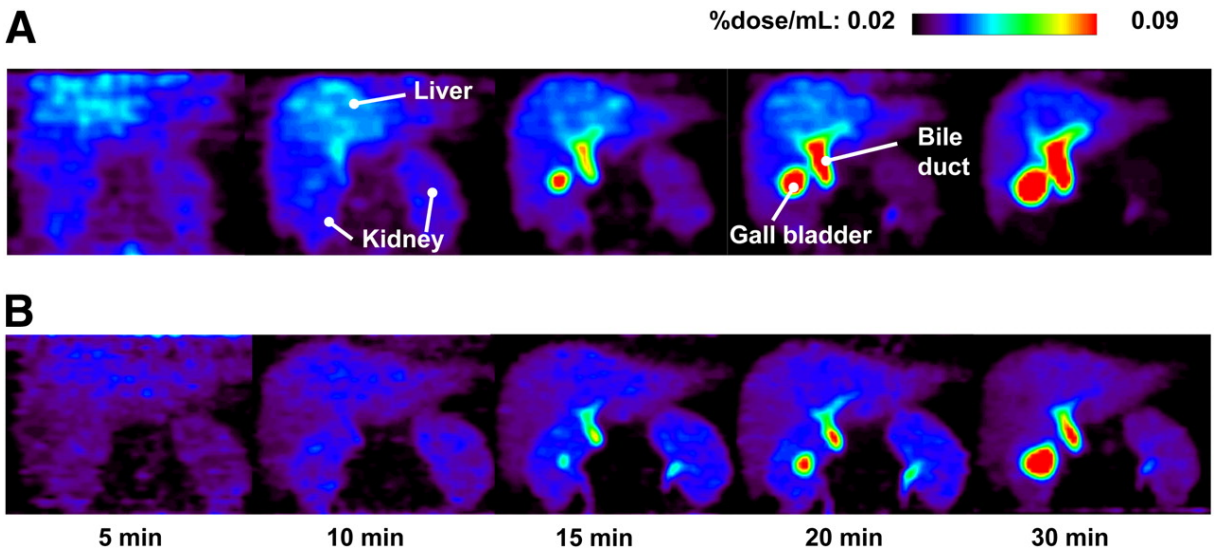
A
%dose/mL: 0.02
0.09
Liver
Kidney
Bile
duct
Gall bladder
B
5 min
10 min
15 min
20 min
30 min

Figure 5